

Identification of potential core genes and miRNAs in pediatric ACC via bioinformatics analysis

Chunyan Fang^{1,§}, Yulong Ye^{2,§}, Fangyue Wang¹, Yifeng Shen¹, Yaodong You^{1,*}

¹TCM Regulating Metabolic Diseases Key Laboratory of Sichuan Province, Hospital of Chengdu University of Traditional Chinese Medicine, Chengdu, Sichuan, China;

²Tea Research Institute, Sichuan Academy of Agricultural Sciences, Chengdu, Sichuan, China.

SUMMARY Pediatric adrenocortical carcinomas (ACC) are rare aggressive neoplasms with heterogeneous prognosis, and often produce a most lethal malignant tumor, whereas its aetiology is still unclear. The aim of the present study was to identify the factors responsible for the development of pediatric ACC, a better understanding of the disease, and investigate new molecular biomarkers and therapeutic targets. To identify the key genes and miRNAs linked to pediatric ACC, as well as their potential molecular mechanisms, the GSEGSE75415 and GSE169253 microarray datasets were analyzed. A total of 329 differentially produced genes (DEGs) and 187 differentially produced miRNAs (DEMs) were obtained after analyzing the GSEGSE75415 and GSE169253 datasets, respectively. Next, 3,359 genes were obtained by overlapping the target mRNAs of DEMs. Following protein-protein interaction network and Gene Ontology analysis, the ten nodes with the highest degrees were screened as hub genes. Among them, the highly expressed hub genes, *MAPK1* and *EP300*, were associated with a worse overall survival. Additionally, hsa-miR-376, hsa-miR-148, hsa-miR-139, and hsa-miR-1305 were strongly associated with poorer survival. We proposed that the hub genes (*MAPK1*, *EP300*, hsa-miR-376, hsa-miR-148, hsa-miR-139, and hsa-miR-1305) may have a definite impact on cellular proliferation and migration in adrenocortical tumors. The roles of these hub genes in adrenocortical tumors may provide novel insight to improve the diagnosis and treatment of patients with pediatric ACC.

Keywords pediatric adrenocortical carcinomas, hub genes, DEGs, microRNAs, prognosis

1. Introduction

Almost 3% to 10% of the population has been reported to present adrenal tumors, and most adrenal tumors are benign (1,2). Conversely, ACCs originating in the outer part of the adrenal gland, are an ultra-rare endocrine malignancy, and lethal malignancies with poor overall survival (3). The highest incidence of ACC is age 1 to 4, and 40 to 50 in two time periods of life. Adult ACC is a rare cancer with a reported incidence of 0.7-2 cases per million people/year worldwide (4). Pediatric ACC is even rarer with a reported incidence of 0.2-0.3 cases per million people/year worldwide (5). Because of its rarity, pediatric ACC is less studied than adult ACC, which may be an obstacle to conducting clinical trials and determining accurate guidelines for the clinical management of pediatric ACC.

ACC in children present as a unique entity, signs and symptoms hyperfunctioning, because of the hypersecretion of sex hormones, cortisol, or aldosterone

hypersecretion or mixed endocrine syndromes (6,7). It has been reported that pediatric ACC more often has a cancer predisposing familial genetic basis, such as the Li-Fraumeni syndrome, the germline P53 mutations, carney complex, and the Beckwith-Wiedemann syndrome (6). The most important treatment of ACC is surgery which is the only mode of therapy documented as effective for treating pediatric ACC, and moreover several adjuvant therapies are used depending on grade and stage of the tumor to lengthen overall survival (8). Unfortunately, the prognosis of ACC is still usually poor due to the late stage at diagnosis. Thus, it is necessary to identify accurate biomarkers for pediatric ACC treatment to facilitate the accurate early stages of diagnosis for the pediatric ACC cases, and therefore for the early discovery and treatment of pediatric ACC cases.

MicroRNAs (miRNAs) are small non-coding regulatory RNA molecules 19 to 25 nucleotides in size that regulate post-transcriptional repression of target genes. A single miRNA can target hundreds of mRNAs

by recognizing the 3'untranslated region (UTR) of target miRNAs. Studies have shown that about 60% of human genes are regulated by miRNAs, indicating that miRNA play key roles in a variety of processes, such as embryogenesis, maintenance of tissue homeostasis, tissue repair and carcinogenesis. And the great majority of studies have found that the abnormal expression of miRNAs correlates with a greater risk of carcinogenesis, including colon cancer, breast cancer, prostate cancer, lung cancer, cholangiocarcinoma, uterine leiomyoma, ovarian cancer, *etc.* (9). Hence, it is urgent and necessary to explore novel therapeutic targets for the treatment of pediatric ACC

In the present study, we selected two gene expression datasets (GSEGSE75415, and GSE169253), which were downloaded from the Gene Expression Omnibus (GEO) database, to obtain differentially expressed genes (DEGs) and differentially expressed microRNAs (DEMs) between pediatric adrenocortical tumors and normal adrenal glands. Differentially expressed miRNAs were identified by integrating multiple bioinformatics analysis methods. Then, functional enrichment and network analyses were applied to identify target genes of differentially expressed miRNAs. Subsequently, we established a protein-protein interaction (PPI) network to identify hub genes related to ACC. The expression values of these hub genes were determined using the online database UALCAN. Survival analysis of these hub genes was performed using the online database Gene Expression Profiling Interactive Analysis (GEPIA). Our findings serve as a valuable resource to further explore the mechanisms of pediatric ACC development and progression, and provide potentially effective diagnostic markers and therapeutic targets for pediatric ACC.

2. Materials and Methods

2.1. Identification of DEGs and DEMs

Two gene expression profiles, [GSE75415](https://www.ncbi.nlm.nih.gov/geo/) and [GSE169253](https://www.ncbi.nlm.nih.gov/geo/), were obtained from the GEO database (<http://www.ncbi.nlm.nih.gov/geo/>). The array data of GSE75415 comprising 24 pediatric tumors and 7 normal adrenal glands was submitted by West AN *et al.* (10). [GSE169253](https://www.ncbi.nlm.nih.gov/geo/) consisted of 37 adrenocortical tumors and 9 non-neoplastic adrenal controls contributed by Veronez LC *et al.* (11). DEGs were obtained from the GEO database by GEO2R analysis (<http://www.ncbi.nlm.nih.gov/geo/geo2r/>). Adjusted $p < 0.05$ and log fold-change ($|\log FC| > 2.0$) were set as the DEG cutoff criterion. Adjusted $p < 0.05$ and $|\log FC| > 1.0$ were set as the DEM cutoff criterion.

2.2. Target prediction of the DEMs and screening of the key oncogenes

The online tool miRDB (<http://mirdb.org/>) and

TargetScanHuman 7.2 (https://www.targetscan.org/vert_72/) were used to predict the mRNAs potentially targeted by the DEMs acquired from the [GSE169253](https://www.ncbi.nlm.nih.gov/geo/) dataset. The criterion of any target was a matching score = 1. The intersection of all targets was obtained through a Venn diagram. Given all DEMs were downregulated, we screened all the upregulated DEMs from the [GSE75415](https://www.ncbi.nlm.nih.gov/geo/) dataset. The intersection of DEGs and the targets of DEMs represented the key oncogenes associated with ACC.

2.3. Gene Ontology (GO) and Encyclopedia of Genes and Genomes (KEGG) enrichment analysis

GO analysis is a commonly used method for large-scale functional enrichment research; gene functions can be classified into biological process (BP), molecular function (MF) and cellular component (CC). KEGG is a widely used database that stores data on genomes, biological pathways, diseases, chemical substances and drugs. GO annotation and KEGG pathway enrichment analyses of the DEGs identified in this study were performed using DAVID tools. $p < 0.05$ was considered to indicate a statistically significant difference.

2.4. Protein-protein interaction (PPI) enrichment analysis

PPI enrichment analysis was carried out on the key oncogenes using the Search Tool for the Retrieval of Interacting Genes/Proteins (STRING) database (<https://string-db.org/>), and a PPI network was generated. Only physical interactions (physical score > 0.4) in STRING were used. Subsequently, the PPI network was visualized by Cytoscape software (version 3.7.1; www.cytoscape.org/). Nodes with a higher degree of connectivity tend to be more essential in maintaining the stability of the entire network. CytoHubba (version 0.1) (12), a plugin in Cytoscape, was used to calculate the degree of each protein node. In our study, the top ten genes were identified as hub genes.

2.5. Expression profiles of hub genes based on tumor histology and survival analysis

UALCAN (<http://UALCAN.path.uab.edu>) and GEPIA (<http://gepia.cancer-pku.cn/>) are user-friendly, interactive web resource for analyzing cancer transcriptome data. According to the median expression of a particular gene, the patients with ACC were split into high and low expression groups. The overall survival (OS) of ACC patients was evaluated using GEPIA (13). $p < 0.05$ was considered to indicate a statistically significant result.

2.6. Exosomal miRNA-mRNA network model construction

By using miRDIP v4.1 online tool, the interactions

between the key mRNAs and key exosomal miRNAs were obtained. Then, the interactions showing high confidence class were chosen for construction of exosomal miRNA-mRNA network by using Cytoscape v3.7.2. The mRNAs in the network were considered as hub mRNAs in this study.

3. Results

3.1. ACC-associated DEGs and DEMs

The gene expression profiles GSE75415 and GSE169253 were selected in this study. Based on the criteria of $P < 0.05$ and $|\log_2FC| > 2.0$, a total of 329 DEGs were identified from GSE75415. Of these, 125 were up-regulated, and 204 were down-regulated in pediatric tumors compared with normal adrenals (Figure 1A). A total of 106 DEMs are upregulated, and 81 DEMs are down-regulated in adrenocortical tumors (Figure 1B). All of these DEMs were identified from GSE169253. We selected five up-regulated DEMs and down-regulate DEMs respectively as hub exosomal miRNAs, with the largest differential multiples, to predict miRNA target genes (Table 1).

3.2. Target genes of the DE miRNAs

In order to reduce the false positive rate of software prediction results, the targets of the above 10 miRNAs were acquired by two miRNA target prediction softwares, miRDB and TargetscanHuman7.2. The results show that there are 10, 29, 138, 298 and 505 target genes in five up-regulated miRNA, hsa-miR-1915-5p, hsa-miR-615-5p, hsa-miR-587, hsa-miR-611 and hsa-miR-452-3p, respectively (Figure 2); There are 393, 293, 15, 1526 and 152 target genes in five down-regulated miRNA, hsa-miR-630, hsa-miR-575, hsa-miR-572, hsa-miR-1305 and hsa-miR-139-3p, respectively (Figure 3).

3.3. Functional and pathway enrichment analyses of target genes

The functional categories of the identified proteins were analyzed with Blast2GO software based on their Gene Ontology (GO) annotations. The enriched GO terms were divided into Biological Processes (BP), Cellular Component (CC), and Molecular Function (MF) ontology terms. The 921 genes identified in five up-regulated miRNAs could be classified into 1,472 categories based

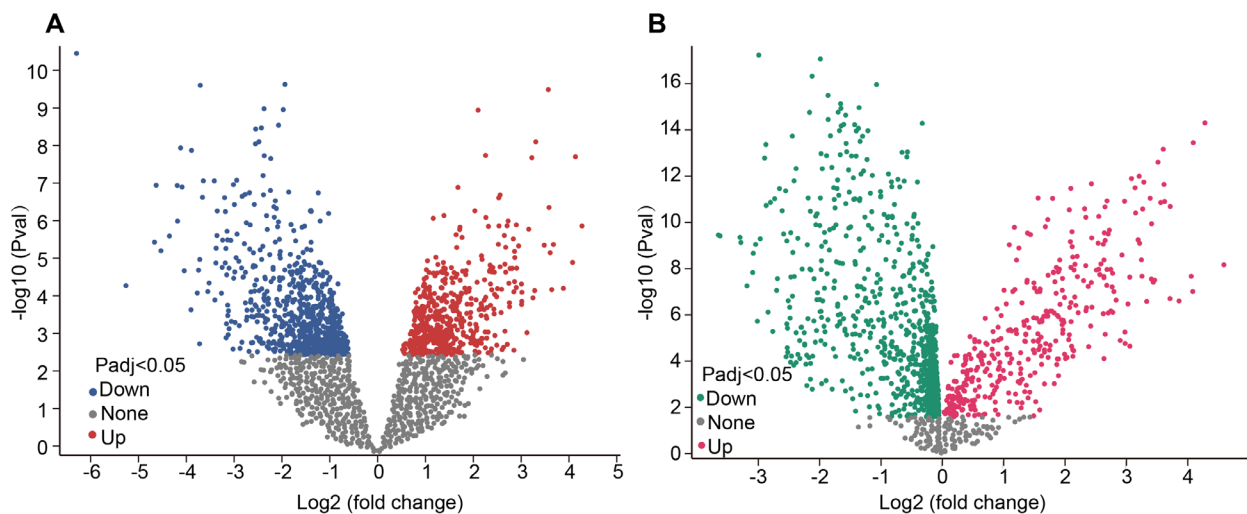


Figure 1. Volcano plots of differentially expressed mRNAs (DE mRNAs, in the GSE75415 dataset) (A), and miRNA (DE-miRs, in the 169253 dataset) (B). DE, differentially expressed.

Table 1. The largest differential expression of miRNA in adrenocortical tumors and non-neoplastic adrenal controls

Items	miRNA_ID	log ₂ (fold change)	adj. p value	p value
Up-regulated miRNA	hsa-miR-376a	4.605	1.06E-07	8.12E-09
	hsa-miR-21	4.296	1.30E-12	6.45E-15
	hsa-miR-376c	4.073	1.04E-06	1.13E-07
	hsa-miR-377	4.073	2.81E-07	2.52E-08
	hsa-miR-148a	3.73	7.15E-10	2.52E-11
Down-regulated miRNA	hsa-miR-630	-3.635	7.91E-09	4.25E-10
	hsa-miR-575	-3.283	9.65E-09	5.37E-10
	hsa-miR-572	-3.076	2.03E-07	1.74E-08
	hsa-miR-1305	-3.067	3.82E-08	2.59E-09
	hsa-miR-139-3p	-2.977	1.57E-14	7.92E-18

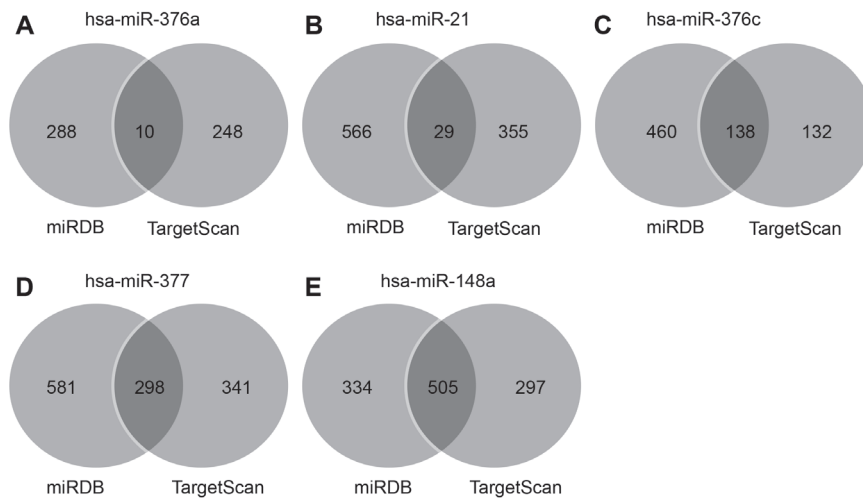


Figure 2. Target gene prediction of five miRNA with the largest up-regulated expression.

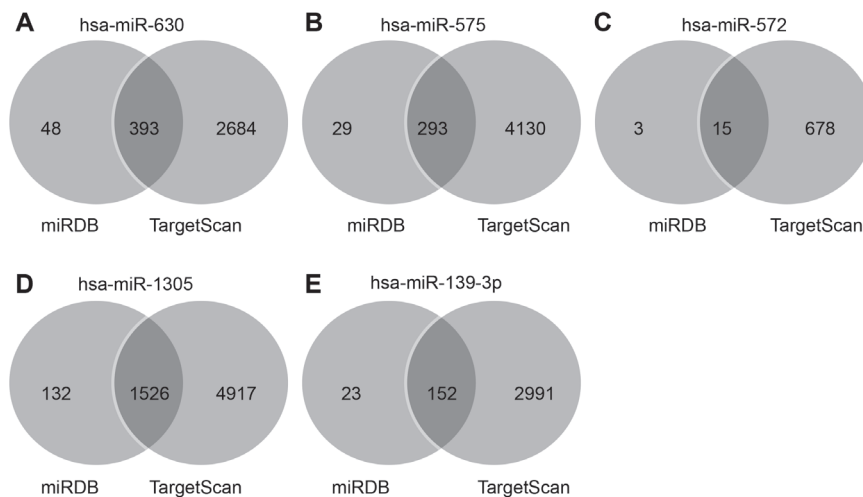


Figure 3. Target gene prediction of five miRNAs with the largest down-regulated expression.

on their annotated BP, and most of them were distributed in neuron projection development, vasculature development, neuron projection morphogenesis, plasma membrane bounded cell projection morphogenesis, cell projection morphogenesis, cell part morphogenesis, blood vessel development, cell morphogenesis, cellular component morphogenesis, and tube morphogenesis, implying that these processes play a significant roles for the occurrence of ACC in children. For CC, the postsynapse, axon, neuron to neuron synapse, dendrite, asymmetric synapse, and dendritic tree were the largest groups of genes. DNA-binding transcription activator activity, RNA polymerase II-specific, DNA-binding transcription activator activity, phosphotransferase activity, alcohol group as acceptor, protein kinase activity, and kinase activity were the most abundant MF categories, which implied that transcription activator activity and kinase activity are vital for carcinogenesis of ACC (Table 2).

The results of GO analysis indicated that the target genes of down-regulated miRNAs were mainly enriched

in BPs, including head development, brain development, neuron projection development, and cell morphogenesis. CC analysis showed that the target genes of down-regulated miRNAs were significantly enriched in Golgi apparatus subcompartment axon, cytoplasmic stress granule, and intracellular protein-containing complex. For MF ontology, these genes were mainly enriched in chromatin binding, protein domain specific binding, nucleoside-triphosphatase activity, and kinase activity (Table 3).

To obtain an overview of the function of target genes of DEMs, the gene identifications were used to search KEGG pathway database using KAOBAS 2.0. The genes involved in Pathways in cancer, PI3K-Akt signaling pathway, Breast cancer, Proteoglycans in cancer, FoxO signaling pathway and MAPK signaling pathway were the most abundant pathways of the target genes of up-regulated DEMs (Figure 4A). Nevertheless, the target genes of down-regulated DEMs were also mainly enriched in FoxO signaling pathway, Pathways in cancer, PI3K-Akt signaling pathway, MAPK signaling pathway,

Table 2. Significantly enriched Go terms of the target genes of up-regulated miRNAs

Category	Term	Description	Count	p value
BP term	GO:0031175	neuron projection development	641	1E-23
	GO:0001944	vasculature development	526	1E-22
	GO:0048812	neuron projection morphogenesis	454	1E-21
	GO:0120039	plasma membrane bounded cell projection morphogenesis	458	1E-21
	GO:0048858	cell projection morphogenesis	462	1E-21
	GO:0032990	cell part morphogenesis	481	1E-20
	GO:0001568	blood vessel development	505	1E-20
	GO:0000902	cell morphogenesis	670	1E-19
	GO:0032989	cellular component morphogenesis	574	1E-19
	GO:0035239	tube morphogenesis	663	1E-19
CC term	GO:0098794	postsynapse	614	1E-19
	GO:0030424	axon	631	1E-19
	GO:0098984	neuron to neuron synapse	347	1E-17
	GO:0030425	dendrite	611	1E-15
	GO:0032279	asymmetric synapse	323	1E-15
	GO:0097447	dendritic tree	613	1E-15
	GO:0099572	postsynaptic specialization	341	1E-15
	GO:0097060	synaptic membrane	373	1E-14
	GO:0014069	postsynaptic density	318	1E-14
	GO:0048471	perinuclear region of cytoplasm	721	1E-13
MF term	GO:0001228	DNA-binding transcription activator activity, RNA polymerase II-specific	462	1E-17
	GO:0001216	DNA-binding transcription activator activity	466	1E-17
	GO:0016773	phosphotransferase activity, alcohol group as acceptor	674	1E-16
	GO:0004672	protein kinase activity	565	1E-16
	GO:0016301	kinase activity	730	1E-15
	GO:0004674	protein serine/threonine kinase activity	430	1E-13
	GO:0019904	protein domain specific binding	687	1E-13
	GO:0004712	protein serine/threonine/tyrosine kinase activity	446	1E-13
	GO:0008134	transcription factor binding	595	1E-12
	GO:0106310	protein serine kinase activity	361	1E-12

Table 3. Significantly enriched Go terms of the target genes of down-regulated miRNAs

Category	Term	Description	Count	p value
BP term	GO:0060322	head development	789	1E-16
	GO:0007420	brain development	744	1E-14
	GO:0031175	neuron projection development	641	1E-14
	GO:0000902	cell morphogenesis	670	1E-12
	GO:0000278	mitotic cell cycle	605	1E-11
	GO:0048812	neuron projection morphogenesis	454	1E-11
	GO:0007017	microtubule-based process	786	1E-11
	GO:1903047	mitotic cell cycle process	514	1E-11
	GO:0051301	cell division	503	1E-11
	GO:0120039	plasma membrane bounded cell projection morphogenesis	458	1E-11
CC term	GO:0098791	Golgi apparatus subcompartment	384	1E-12
	GO:0030424	axon	631	1E-12
	GO:0010494	cytoplasmic stress granule	81	1E-11
	GO:0140535	intracellular protein-containing complex	753	1E-11
	GO:0005813	centrosome	620	7.94328E-10
	GO:0000139	Golgi membrane	662	1.25893E-09
	GO:0016607	nuclear speck	413	3.98107E-09
	GO:0005802	trans-Golgi network	261	3.98107E-09
	GO:0036464	cytoplasmic ribonucleoprotein granule	244	1.99526E-08
	GO:0005819	spindle	425	2.51189E-08
MF term	GO:0003682	chromatin binding	586	1E-11
	GO:0019904	protein domain specific binding	687	1E-10
	GO:0017111	nucleoside-triphosphatase activity	699	1.99526E-10
	GO:0016301	kinase activity	730	3.16228E-10
	GO:0016773	phosphotransferase activity, alcohol group as acceptor	674	5.01187E-10
	GO:0008134	transcription factor binding	595	7.94328E-10
	GO:0070717	poly-purine tract binding	29	1.25893E-09
	GO:0003924	GTPase activity	337	1.58489E-09
	GO:0003712	transcription coregulator activity	497	1.58489E-09
	GO:0016462	pyrophosphatase activity	754	3.16228E-09

and axon guidance (Figure 4B).

3.4. PPI network construction and the analysis of hub genes

A total of 900 nodes and 4,223 edges were mapped in the PPI network of the targets of up-regulated DEMs (Figure 5A). The 10 nodes with the highest degrees, including phosphatase and tensin homolog (*PTEN*), phosphatidylinositol-4,5-bisphosphate 3-kinase catalytic subunit alpha (*PIK3CA*), mitogen-activated protein kinase 1 (*MAPK1*), estrogen receptor 1 (*ESR1*), and erb-b2 receptor tyrosine kinase 3 (*ERBB3*) were screened as hub genes (Table 4).

There were 1,555 nodes and 7,712 edges, which

mapped in the PPI network of the targets of down-regulated DEMs (Figure 5B). The 10 nodes with the highest degrees of these genes were: tumor protein p53 (*TP53*), E1A binding protein p300 (*EP300*), KRAS proto-oncogene, GTPase (*KRAS*), DDB1 and CUL4 associated factor 10 (*DCAF10*), and phosphatase and tensin homolog (*PTEN*) (Table 5).

3.5. Expression profiles of the hub genes and survival analysis

To investigate the expression and prognostic values of the ten potential hub genes, the GEPIA bioinformatics analysis platform was used. We found that the nine hub genes were significantly (all *p*-value < 0.05) associated

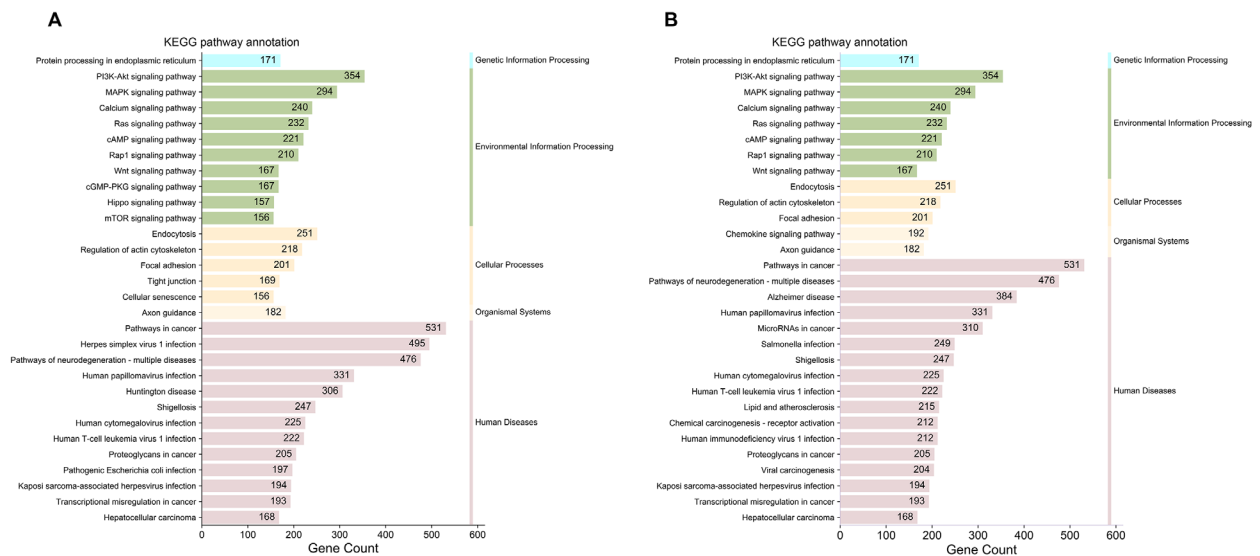


Figure 4. KEGG pathways analysis of identified genes.

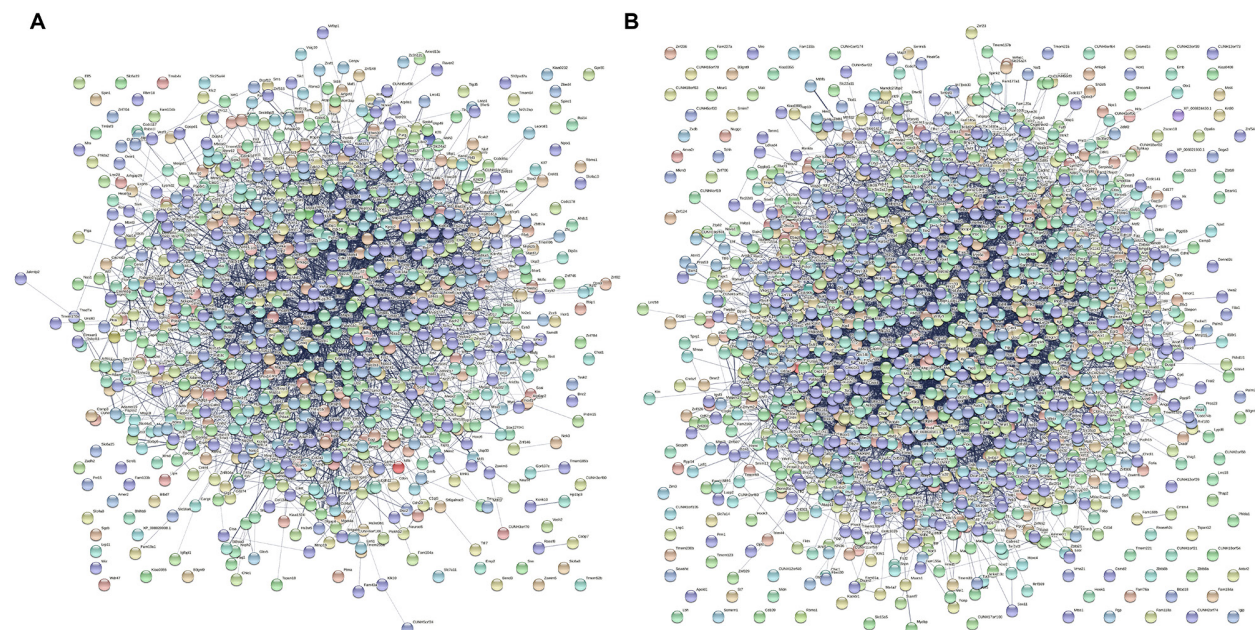


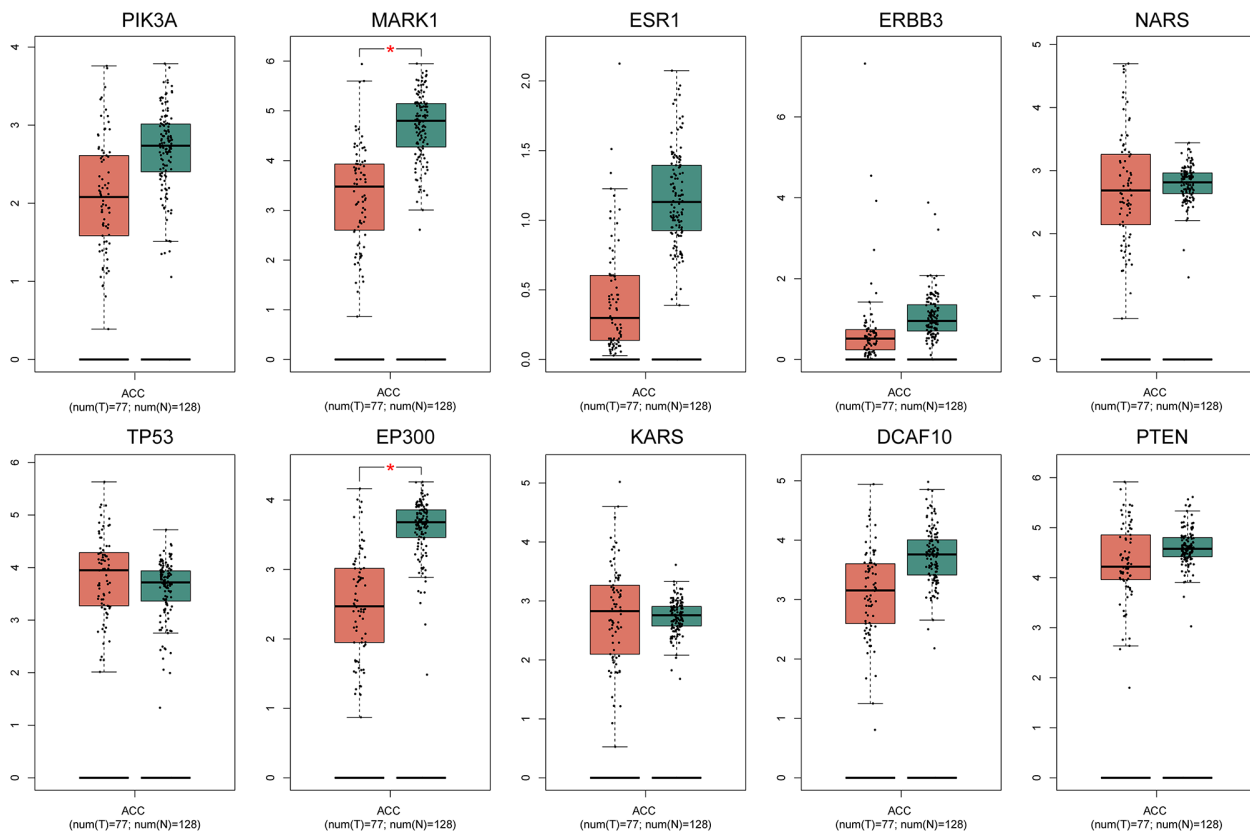
Figure 5. PPI network of the of the target genes of DEMs.

Table 4. Top five key genes with the highest degrees of connectivity in the target genes of up-regulated DEMs

Gene	Gene description	Degree
<i>PIK3CA</i>	phosphatidylinositol-4,5-bisphosphate 3-kinase catalytic subunit alpha	64
<i>MAPK1</i>	mitogen-activated protein kinase 1	63
<i>ESR1</i>	estrogen receptor 1	55
<i>ERBB3</i>	erb-b2 receptor tyrosine kinase 3	54
<i>NRAS</i>	NRAS proto-oncogene, GTPase	52

Table 5. Top five key genes with the highest degrees of connectivity in the target genes of down-regulated DEMs

Gene	Gene description	Degree
<i>TP53</i>	tumor protein p53	137
<i>EP300</i>	E1A binding protein p300	118
<i>KRAS</i>	KRAS proto-oncogene, GTPase	89
<i>DCAF10</i>	DDB1 and CUL4 associated factor 10	80
<i>PTEN</i>	phosphatase and tensin homolog	79

**Figure 6. Gene Expression Profiling Interactive Analysis for overall survival associated with the expression of the ten hub genes in patients with adrenocortical carcinoma. Red line represents high expression, and blue line represents low expression.**

with shorter survival duration of the adrenocortical carcinoma (Figure 6). *MARP1* and *EP300* were significant, and we found that the high expression of hub genes was associated with an unfavorable OS of patients with adrenocortical carcinoma (Figure 7).

3.6. Validation of the hub exosomal miRNAs

As shown in Figure 8A, an exosomal miRNA-mRNA network consisting of four miRNAs (hsa-miR-376, hsa-miR-148, hsa-miR-139, and hsa-miR-1305) and 6

mRNAs (*ESR1*, *PTEN*, *NARS*, *ERBB3*, *MAPK1*, and *KARS*) was constructed. These mRNAs and miRNAs were respectively considered to be hub mRNAs and hub exosomal miRNAs that might play crucial roles in ACC development *via* exosomes. As shown in Figure 8B, every index in different times had no significant difference from that in primary carcinoma ($p > 0.05$). Then, we explored the value of the hub exosomal miRNAs as diagnosis biomarkers in ACC by performing ROC curves and calculating the area under the curves (AUCs) [95% confidence intervals (CIs)]. The AUCs

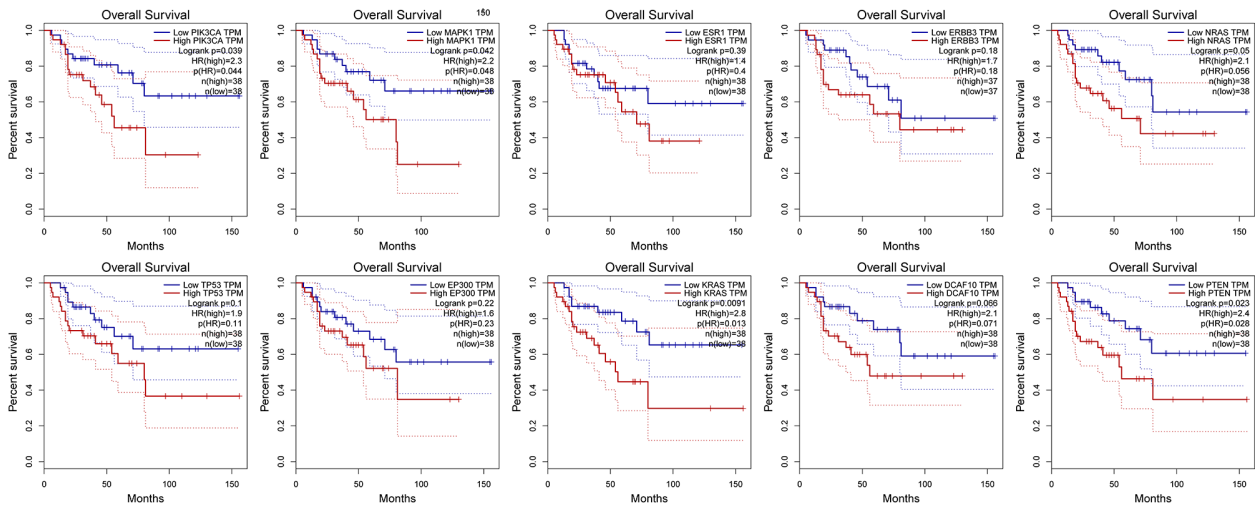


Figure 7. Expression values of the top hub genes in adrenocortical carcinoma and non-adrenocortical carcinoma.

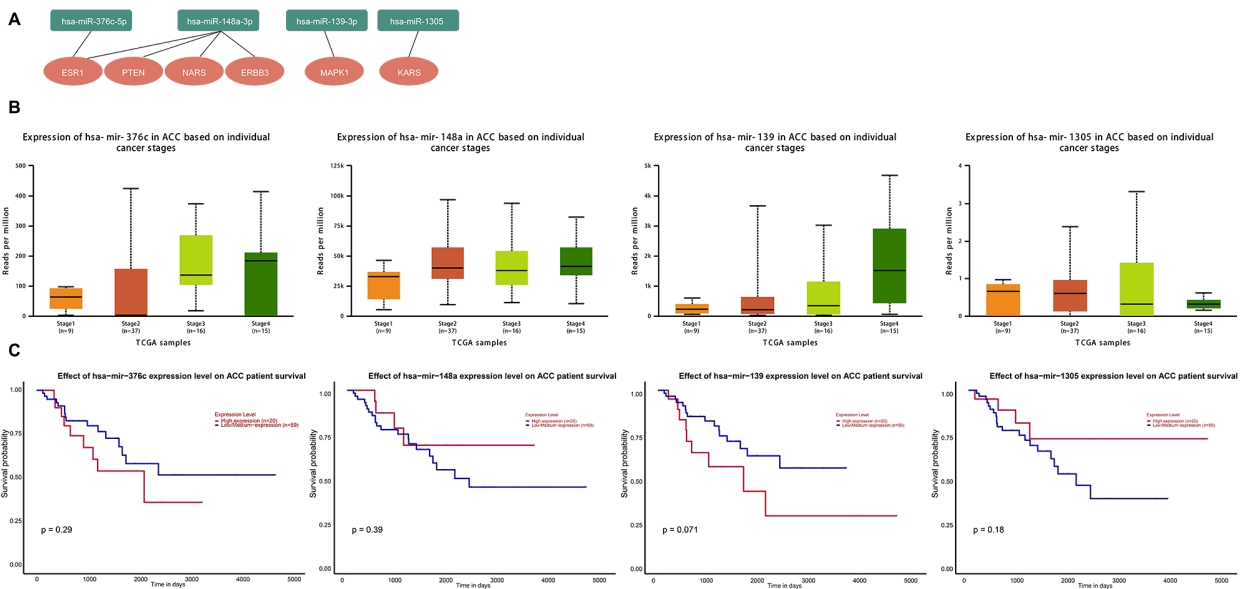


Figure 8. Validation of the hub exosomal miRNAs. A Exosomal miRNA-mRNA network. B Expression of Hub genes in primary ACC and metastatic ACC. C Results for the overall survival (OS) analysis of the hub mRNAs.

of hsa-miR-376, hsa-miR-148, hsa-miR-139, and hsa-miR-1305 were respectively 0.29, 0.39, 0.071, and 0.18, which proved that the four hub exosomal miRNAs can well distinguish tumor and normal samples.

4. Discussion

Pediatric ACC is rare aggressive neoplasms with heterogeneous prognosis, and often is a most lethal malignant tumor. It is usually discovered and diagnosed at its advanced stage. Despite extensive efforts, identifying reliable prognostic factors for pediatric patients with ACC remains a challenge. MicroRNA (miRNA) signatures have been associated with cancer diagnosis, treatment response, and prognosis of several types of cancer. However, the role of miRNAs has been poorly explored in pediatric ACC. Therefore, it

is important to develop a miRNA-mRNA network that drives the mechanisms of pediatric ACC for identifying potential biomarkers for improving the diagnostic accuracy of pediatric ACC.

In this study, through comprehensive analysis of the open access miRNA and mRNA data for pediatric ACC from GEO, we identified 329 DEGs and 187 DEMs that were differentially expressed in pediatric tumors and normal adrenal glands based on the [GSE75415](#) dataset and [GSE169253](#) dataset, respectively. A total of 106 DEMs are upregulated, and 81 DEMs are down-regulated in adrenocortical tumors. All of these DEMs were identified from [GSE169253](#). We selected five up-regulated DEMs and down-regulated DEMs respectively as hub miRNAs, with the largest differential multiples, to predict their target mRNAs. Next, 3,359 genes were obtained by overlapping the target mRNAs, which could

ensure to get the most potential mRNAs associated with pediatric ACC progression. The genes identified in five up-regulated miRNAs were enriched in "neuron projection development", "vasculature development", and "neuron projection morphogenesis", while the genes identified in five down-regulated miRNAs were mainly enriched in "head development", "brain development", and "neuron projection development". Moreover, all these target genes of DEMs were involved in "Pathways in cancer", "PI3K-Akt signaling pathway", "MAPK signaling pathway", and "FoxO signaling pathway". Then, we identified ten high-degree hub genes by constructing the PPI network, including *PIK3CA*, *MAPK1*, *ESR1*, *ERBB3*, *NRAS*, *TP53*, *EP300*, *KRAS*, *DCAF10*, and *PTEN*. We predicted the association between the expression of the hub genes and the prognosis of ACC patients. Based on GEPIA, the overexpression of all hub genes was related to an unfavorable prognosis in patients with ACC. Among them, *MAPK1* and *EP300* were significantly up-regulated in pediatric tumors. Finally, we performed intersection of differentially expressed miRNAs with hub genes. After finishing the intersection, a total of 4 candidate miRNAs were obtained to distinguish tumor and normal samples, including hsa-miR-376, hsa-miR-148, hsa-miR-139, and hsa-miR-1305.

Recent studies have found that MAPK1 is highly expressed in many tumors, including liver cancer, renal cell carcinoma, prostate cancer, lung cancer, and so on (14-17). The abnormal-expression of MAPK in tumors leads to an activation of the MAPK pathway, which is a highly conserved module that is involved in various cellular functions, including cell proliferation, differentiation and migration. This pathway involves besides RAF kinases and upstream GTPases of the RAS family, the mitogen-activated extracellular signal-regulated kinases 1/2 (MEK1/2) and extracellular signal-regulated kinases 1/2 (ERK1/2) (18). It is hyperactivated in a large variety of tumors, and many of its elements have been identified as oncogenes. These observations have generated a profound interest in targeting this pathway as a therapeutic option for cancer (19). *EP300* is known to participate in a variety of cellular functions including DNA repair, cell growth and differentiation, apoptosis, cell cycle regulation and chromatin remodeling, all of which are consistent with a tumor suppressor role (20). *EP300* acetylation of TP53 in response to DNA damage regulates its DNA binding and transcription functions (21). Therefore, *MAPK1* and *EP300* in ACC are worthy of more attention.

Members of the miR-376 cluster are transcribed as one transcript bearing multiple hairpin structures that undergo RNA editing at multiple sites prior to being processed into individual pre-miRNAs. miR-376a has two major editing sites located at +4 in 5p seed sequence and +44 in 3p seed sequence (22,23). These editing sites show high levels of modification frequencies in

specific regions of the brain compared to other tissues. It is consistent with our results that the genes identified in DEMs were mainly enriched in head development and neuron projection development. The altered expression of hsa-miR-148 was found in various tumors, including gastric cancer, pancreatic cancer, lung cancer and gastric cancer, *etc.* (24-27). It has been largely through directly targeting key players of integrin signaling like ITGA5, ROCK1, and PI3KCA/p110 α as well as NRAS, which controlled the pathway involved in tumor growth and metastasis (26). Cristina Montero-Conde reported that differential expression analysis revealed a consistent hsa-miR-139-5p down expression in primary carcinomas from patients with recurrent/metastatic disease compared to disease-free patients, indicating that hsa-miR-139 was associated with recurrent disease independent of genetic background (28). Thus, miRNA differential expression analysis between prognostic classes identify hsa-miR-139-5p as a disease outcome marker. Yinjie Su indicated that circRIP2 sponges miR-1305 to elevate Tgf- β 2 in bladder cancer cells (29). Moreover, Welu reported that ASB16-AS1 promotes cell proliferation, migration, invasion *via* binding miR-1305 with Wnt2, and enhancing the Wnt/ β -catenin pathway in cervical cancer (30).

5. Conclusions

Based on our results and above-mentioned literature, we suppose that there are multiple regulatory axes related to ACC development in intracellular communications mediated by miRNA and mRNA. The current study efficiently identified several candidate targets (*MAPK1*, *EP300*, *hsa-miR-376*, *hsa-miR-148*, *hsa-miR-139*, and *hsa-miR-1305*) that can potentially serve as biomarkers in the diagnosis of pediatric ACC, and may be potential targets for seminoma therapy. These findings provide a new direction for diagnosis and treatment of pediatric ACC.

Funding: This work was supported by the National Natural Science Foundation of China [No. 81973647] and the Xinglin scholar discipline promotion talent program of Chengdu University of traditional Chinese medicine [No. BSH2021018].

Conflict of Interest: The authors have no conflicts of interest to disclose.

References

1. NIH state-of-the-science statement on management of the clinically inapparent adrenal mass ("incidentaloma"). NIH Consens State Sci Statements. 2002; 19:1-25.
2. Thampi A, Shah E, Elshimy G, Correa R. Adrenocortical carcinoma: a literature review. Transl Cancer Res. 2020; 9:1253-1264.
3. Bilimoria KY, Shen WT, Elaraj D, Bentrem DJ,

- Winchester DJ, Kebebew E, Sturgeon C. Adrenocortical carcinoma in the United States: treatment utilization and prognostic factors. *Cancer*. 2008; 113:3130-3136.
4. Else T, Kim AC, Sabolch A, Raymond VM, Kandathil A, Caoili EM, Jolly S, Miller BS, Giordano TJ, Hammer GD. Adrenocortical carcinoma. *Endocr Rev*. 2014; 35:282-326.
 5. Mahendraraj K, Lau CSM, Sidhu K, Chamberlain RS. Adrenocortical carcinoma in adults and children: a population-based outcomes study involving 1,623 patients from the Surveillance, Epidemiology, and End Result (SEER) Database (1973-2012). *Clin Surg*. 2016; 1:1017.
 6. Ribeiro RC, Figueiredo B. Childhood adrenocortical tumours. *Eur J Cancer*. 2004; 40:1117-1126.
 7. Michalkiewicz E, Sandrini R, Figueiredo B, Miranda EC, Caran E, Oliveira-Filho AG, Marques R, Pianovski MA, Lacerda L, Cristofani LM, Jenkins J, Rodriguez-Galindo C, Ribeiro RC. Clinical and outcome characteristics of children with adrenocortical tumors: a report from the International Pediatric Adrenocortical Tumor Registry. *J Clin Oncol*. 2004; 22:838-845.
 8. From the American Association of Neurological Surgeons (AANS), American Society of Neuroradiology (ASNR), Cardiovascular and Interventional Radiology Society of Europe (CIRSE), *et al*. Multisociety consensus quality improvement revised consensus statement for endovascular therapy of acute ischemic stroke. *Int J Stroke*. 2018; 13:612-632.
 9. Lee YS, Dutta A. MicroRNAs in cancer. *Annu Rev Pathol*. 2009; 4:199-227.
 10. West AN, Neale GA, Pounds S, Figueiredo BC, Rodriguez Galindo C, Pianovski MA, Oliveira Filho AG, Malkin D, Lalli E, Ribeiro R, Zambetti GP. Gene expression profiling of childhood adrenocortical tumors. *Cancer Res*. 2007; 67:600-608.
 11. Veronez LC, Fedatto PF, Correa CAP, *et al*. MicroRNA expression profile predicts prognosis of pediatric adrenocortical tumors. *Pediatr Blood Cancer*. 2022; 69:e29553.
 12. Chin CH, Chen SH, Wu HH, Ho CW, Ko MT, Lin CY. cytoHubba: identifying hub objects and sub-networks from complex interactome. *BMC Syst Biol*. 2014;8 Suppl 4:S11.
 13. Tang Z, Li C, Kang B, Gao G, Li C, Zhang Z. GEPIA: a web server for cancer and normal gene expression profiling and interactive analyses. *Nucleic Acids Res*. 2017; 45:W98-W102.
 14. Hu ZQ, Zhou SL, Li J, Zhou ZJ, Wang PC, Xin HY, Mao L, Luo CB, Yu SY, Huang XW, Cao Y, Fan J, Zhou J. Circular RNA sequencing identifies circASAP1 as a key regulator in hepatocellular carcinoma metastasis. *Hepatology*. 2020; 72:906-922.
 15. Hao JF, Chen P, Li HY, Li YJ, Zhang YL. Effects of LncRNA HCP5/miR-214-3p/MAPK1 molecular network on renal cell carcinoma cells. *Cancer Manag Res*. 2020; 12:13347-13356.
 16. Hu D, Jiang L, Luo S, Zhao X, Hu H, Zhao G, Tang W. Development of an autophagy-related gene expression signature for prognosis prediction in prostate cancer patients. *J Transl Med*. 2020; 18:160.
 17. Zhang ZY, Gao XH, Ma MY, Zhao CL, Zhang YL, Guo SS. CircRNA_101237 promotes NSCLC progression *via* the miRNA-490-3p/MAPK1 axis. *Sci Rep*. 2020; 10:9024.
 18. Kunz M. Oncogenes in melanoma: an update. *Eur J Cell Biol*. 2014; 93:1-10.
 19. Drosten M, Barbacid M. Targeting the MAPK pathway in KRAS-driven tumors. *Cancer Cell*. 2020; 37:543-550.
 20. Gayther SA, Batley SJ, Linger L, Bannister A, Thorpe K, Chin SF, Daigo Y, Russell P, Wilson A, Sowter HM, Delhanty JD, Ponder BA, Kouzarides T, Caldas C. Mutations truncating the EP300 acetylase in human cancers. *Nat Genet*. 2000; 24:300-303.
 21. Yuan ZM, Huang Y, Ishiko T, Nakada S, Utsugisawa T, Shioya H, Utsugisawa Y, Yokoyama K, Weichselbaum R, Shi Y, Kufe D. Role for p300 in stabilization of p53 in the response to DNA damage. *J Biol Chem*. 1999; 274:1883-1886.
 22. Yang Y, Okada S, Sakurai M. Adenosine-to-inosine RNA editing in neurological development and disease. *RNA Biol*. 2021; 18:999-1013.
 23. Kawahara Y, Zinshteyn B, Sethupathy P, Iizasa H, Hatzigeorgiou AG, Nishikura K. Redirection of silencing targets by adenosine-to-inosine editing of miRNAs. *Science*. 2007; 315:1137-1140.
 24. Nie F, Liu T, Zhong L, Yang X, Liu Y, Xia H, Liu X, Wang X, Liu Z, Zhou L, Mao Z, Zhou Q, Chen T. MicroRNA-148b enhances proliferation and apoptosis in human renal cancer cells *via* directly targeting MAP3K9. *Mol Med Rep*. 2016; 13:83-90.
 25. Liu GL, Liu X, Lv XB, Wang XP, Fang XS, Sang Y. miR-148b functions as a tumor suppressor in non-small cell lung cancer by targeting carcinoembryonic antigen (CEA). *Int J Clin Exp Med*. 2014; 7:1990-1999.
 26. Cimino D, De Pittà C, Orso F, *et al*. miR148b is a major coordinator of breast cancer progression in a relapse-associated microRNA signature by targeting ITGA5, ROCK1, PIK3CA, NRAS, and CSF1. *FASEB J*. 2013; 27:1223-1235.
 27. Friedrich M, Pracht K, Mashreghi MF, Jäck HM, Radbruch A, Seliger B. The role of the miR-148/-152 family in physiology and disease. *Eur J Immunol*. 2017; 47:2026-2038.
 28. Montero-Conde C, Graña-Castro O, Martín-Serrano G, *et al*. Hsa-miR-139-5p is a prognostic thyroid cancer marker involved in HNRNPF-mediated alternative splicing. *Int J Cancer*. 2020; 146:521-530.
 29. Su Y, Feng W, Shi J, Chen L, Huang J, Lin T. circRIP2 accelerates bladder cancer progression *via* miR-1305/Tgf- β 2/smad3 pathway. *Mol Cancer*. 2020; 19:23.
 30. Liu W, Zhuang R, Feng S, Bai X, Jia Z, Kapora E, Tan W. Long non-coding RNA ASB16-AS1 enhances cell proliferation, migration and invasion *via* functioning as a ceRNA through miR-1305/Wnt/ β -catenin axis in cervical cancer. *Biomed Pharmacother*. 2020; 125:109965.

Received June 27, 2022; Revised August 14, 2022; Accepted August 23, 2022.

[§]These authors contributed equally to this work.

*Address correspondence to:

Yaodong You, TCM Regulating Metabolic Diseases Key Laboratory of Sichuan Province, Hospital of Chengdu University of Traditional Chinese Medicine, No. 39 shi-er-qiao Road, Chengdu, Sichuan 610072, China.

E-mail: yyd110@163.com

Released online in J-STAGE as advance publication August 30, 2022.